



## Acid Adsorption on the Activated Charcoal Synthesized from Low Cost Agricultural Waste under Varying Condition

P. Chaithra, K. Hemashree and J. I. Bhat \*

Department of Chemistry, Mangalore University, Mangalagangothri-574199, India

### PAPER INFO

#### Paper history:

Received 23 February 2017

Accepted in revised form 25 March 2017

#### Keywords:

Acetic acid  
Agricultural waste  
Activated carbon  
Characterization  
Adsorption

### ABSTRACT

The activated charcoal (AC) was synthesized from banana leaf rim (BLR) through three activation methods; physical (BLRC), chemical (Z BLRC, zinc chloride) and microwave activation (MW BLRC). The AC was characterised using powder X-ray diffraction (XRD) and field emission scanning electron microscope (FE-SEM). The Z BLRC has better adsorbent character compared to BLRC or MW BLRC. Adsorption of acetic acid (AA) onto synthesized activated charcoals (BLRC, Z BLRC & MW BLRC) were performed. This experimental data satisfied Freundlich adsorption isotherm equations. Second-order kinetics study holds good for the present adsorption system. Thermodynamic parameters were evaluated. Based on the result it may be concluded that chemical activated charcoal has maximum adsorption efficiency among the three synthesized types of carbons.

doi: 10.5829/idosi.ijee.2017.08.01.07

### INTRODUCTION

The organic acids namely formic acid, acetic acid, oxalic acid, maleic acid, citric acid, phenol etc., are most commonly found in wastewater discharged from various chemical, pharmaceutical, food industries etc. Among these acetic acid is one of the most widely used organic acid in industries [1]. Researchers have found that adsorption onto activated carbon is most widely used and efficient method for the removal of acetic acid from aqueous solution. Activated carbon (AC) is one of the adsorbent having large surface area, active pore sites, surface functional groups and surface charges [2-4]. Researchers have synthesized the activated carbon from cassava peels [5], rice husk [6], cocoa pod [7], date pits [8] etc. The production of activated carbon from green waste will help in its requirement in industry and will reduce agro-waste disposable problem there by cleaning the environment. Banana (*Musa Acuminata Colla*) plant has an origin from India and eastern Asian region (Malayasia and Japan). After harvesting banana fruit bunch from the plant the dried leaf rims will become waste in agricultural field. The literature reveals that banana leaf waste showed 28.5, 24.57 and 9.7% of

cellulose, hemicellulose and lignin, respectively [9]. Banana empty fruit bunch have cellulose, hemicellulose and lignin contents (8.3%, 21.23% and 19.06%, respectively) [10]. The lignocellulosic contents of banana stem are 44.0% for cellulose, 17.5% for hemicellulose, and 37.3% for lignin [11]. The percentage of cellulose, hemicellulose and lignin content was found to be different in the different parts of banana plant. Hence the present study was undertaken using banana leaf rim as a raw material for the activated charcoal preparation.

In this study, we report the synthesis, characterization, evaluation and comparison of adsorption of acetic acid (AA) onto synthesized carbon from banana leaf rim (BLR) by physical (BLRC), chemical (Z BLRC) and microwave (MW BLRC) activation methods. The experimental data fits in to Freundlich and Langmuir adsorption isotherms. The data were tested for first-order and second-order kinetic models. Thermodynamics of adsorption was obtained to know the nature of adsorption process.

### MATERIAL AND METHODS

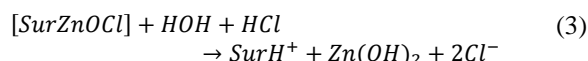
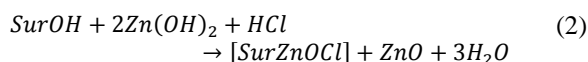
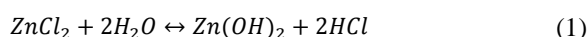
#### Synthesis methods of activated charcoal physical activation

\* Corresponding author: J. Ishwara Bhat  
E-mail: [bhatij@yahoo.com](mailto:bhatij@yahoo.com)

Weighed 20g of dried small pieces of uniform sized banana leaf rim to a petridish. It was heated in hot air oven at 250 °C for 8h. In order to become char BLR sample was heated in muffle furnace at 300°C for 2h. The obtained activated charcoal was crushed in mortar to become powder.

### Chemical activation

The small pieces of hot air oven dried banana leaf rims (20g) was soaked in 200ml of 1M zinc chloride solution (ZnCl<sub>2</sub>) and this mixture was kept in hot plate at 80 °C for 1h stirred with glass rod. After heating it was cooled to room temperature and kept for 24h. Excess ZnCl<sub>2</sub> solution was filtered off and the soaked banana leaf rims were dried under oven at 100 °C for 24h. This was heated in muffle furnace at 300 °C for 2h to get zinc chloride activated banana leaf rim charcoal. Such obtained activated carbon was washed twice with distilled water to remove traces of zinc chloride remained on the surface of the activated charcoal. The chemical activation process involves following steps [12]:



### Microwave activation

20g of hot air oven dried banana leaf rim were grinded in electric mixer grinder to get homogeneous powder and it was activated in domestic microwave oven of the radiation 80 W for a period of 280 minutes. The obtained AC was sieved to uniform size (250 μm) for the adsorption studies.

### Chemicals

The adsorbate used in the present work is acetic acid glacial 99-100% (AR) (Merk specialities Pvt. Ltd., Mumbai, India). Sodium hydroxide pellets extrapure AR and Zinc chloride pure (Sisco Research Laboratories Pvt. Ltd., Mumbai, India).

### Characterization of AC

#### Powder XRD analysis of AC

Physical nature of the synthesized activated charcoal (BLRC, Z BLRC and MW BLRC) was obtained from powder X-ray diffractometer (Rigaku Miniflex 600 diffractometer) using Cu-Kα (λ=1.5418 Å) operating voltage=40 KV and a current of 15 mA. The diffraction angle range was 2θ=10° to 70°.

#### FE-SEM analysis of AC

Banana leaf rim activated charcoal (BLRC, Z BLRC and MW BLRC) were first dried in hot air oven at 105°C for 1h. to remove moisture from the surface. Then it was placed in a desiccator. The dried and powdered activated charcoal samples were sprayed on a carbon tape mounted on an aluminum stub. The surface image was scanned using Carl Zeiss field emission scanning electron microscope. The SEM magnification was 2.50 KX and EHT=5.00kV.

### Adsorption studies

Weighed 0.25 g of activated charcoal samples (BLRC, Z BLRC & MW BLRC ) to a three different conical flask containing 50 ml of 0.05 M acetic acid solution. This was stirred for 30 min on a magnetic stirrer. The concentration of acetic acid solution after the adsorption process was determined by titrometric method. The amount of acetic acid adsorbed (q<sub>e</sub>) was calculated using following equation [13]:

$$q_e = \frac{(C_0 - C_e)W}{w} V \quad (4)$$

Where C<sub>0</sub> is the initial concentration of acetic acid (M); C<sub>e</sub> is the concentration of AA in the solution after adsorption (M); W is the equivalent weight of acid (g.mol<sup>-1</sup>); V is the volume of the solution (ml); and w is the weight of activated carbon (g). The adsorption data fitted with adsorption isotherms namely Freundlich and Langmuir adsorption isotherms. Also kinetics and thermodynamics of adsorption were studied to determine the mechanism of adsorption.

## RESULTS AND DISCUSSION

### Powder XRD analysis of AC

Powder X-Ray pattern of all the three samples obtained and are shown in Figure 1. XRD pattern revealed that chemical activated charcoal is of relatively more amorphous compared either to physical or microwave activated carbon. The angle of diffraction (2θ) and inter planar distance (d) values were obtained from this experiment which were used to evaluate miller indices (hkl) and such resulted data are shown in Figure 1.

Here it can be noticed the shift in the peak from 18.72 (2θ) for Z BLRC to 22.62 (2θ) for chemical activated charcoal. The shift in 2θ (amorphous to crystalline) is probably due to the chemical reaction occurred between carbon and zinc chloride (Eqs. 1, 2 and 3). The crystallite size which is obtained from Scherer's formula [14]:

$$D = \frac{K\lambda}{\beta \cos\theta} \quad (5)$$

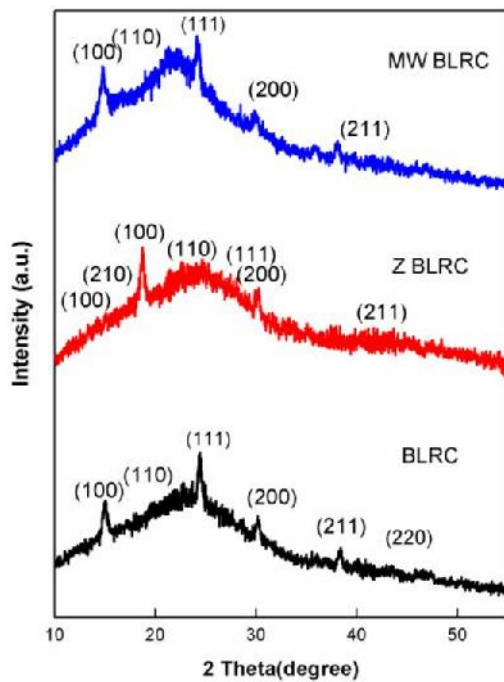


**Figure 1.** XRD pattern of BLRC, Z BLRC and MW BLRC

Where  $K=0.9$ ,  $\lambda=1.5418 \text{ \AA}$  and  $\beta = \text{FWHM}$  in radian. Defect density and lattice strain were calculated by the following equation [15]:

$$\delta = \frac{1}{D^2} \quad (6)$$

$\delta$  is the crystal defect density and  $D$  is the crystallite size or grain size.

$$\eta = \frac{\beta}{4 \tan \theta} \quad (7)$$

Where  $\eta$  is the lattice strain,  $\beta$  is the full width at half maximum and  $\theta$  is the X-ray diffraction angle. Crystallinity index (CrI) was calculated using following equation [16]:

$$CrI = 100 \times \left[ \frac{I_c - I_a}{I_c} \right] \quad (8)$$

In which  $I_c$  is the intensity of crystalline portion and  $I_a$  is the intensity of amorphous peak. Crystallite size ( $D$ ), defect density ( $\delta$ ), lattice strain ( $\eta$ ) and crystallinity index (CrI) values of BLRC, Z BLRC & MW BLRC was shown in Table 1.

The presence of zinc ion on the surface of Z BLRC may be the reason for increase in crystallite size of ZBLRC than BLRC. The defect density was found to be maximum in BLRC is due to the thermal degradation which probably modified nature of the surface. From the evaluation of crystalline index, result obtained was

chemical activated charcoal has more amorphous in nature than crystalline nature.

**TABLE 1.** Crystallite size ( $D$ ), defect density ( $\delta$ ), lattice strain ( $\eta$ ) and crystallinity index (CrI) values of BLRC, Z BLRC and MW BLRC

Samples	$D(\text{\AA})$	$\delta (\text{\AA})^{-2}$	$\eta$	CrI
BLRC	3.9306	0.0647	0.4173	37.8947
Z BLRC	4.1193	0.0589	0.5178	27.5362
MWBLRC	4.4720	0.0500	0.3709	30.0380

### FE-SEM Analysis of AC

The surface morphological changes observed in activated carbons before and after adsorption was shown in Figures 2a to 2f. Figure 2 (a, c and e) shows the surface of three activated carbon before adsorption. Figures 2b, 2d and 2f are of after adsorption. The important observation made was the retention of cellular or fibrous nature of surface. Since activated charcoal derived from plant origin the plant cell wall contains cellulose, hemicellulose and lignin material [17]. Pores having different sizes were observed on the surface of BLRC & Z BLRC (Figures 2a and 2c) and those pores were blocked during adsorption (Figures 2b and 2d). The surface structure of MW BLRC was rough (Figure 2e) and uneven distribution of porous was observed. The nature of surface changed after adsorption process (Figure 2f). Also XRD pattern of Z BLRC (Figure 1) shows more amorphous nature than crystalline nature. Therefore, from both characterization XRD and SEM it is clear that Z BLRC has good adsorbent characteristics than BLRC & MW BLRC.

### Adsorption studies

#### Effect of Activated charcoal size and weight on adsorption

Effect of AC size (53, 106, 212 and 250  $\mu\text{m}$ ) on adsorption of AA was studied. Weighed 0.25 g of activated charcoal (BLRC, Z BLRC and MW BLRC) to different reagent bottles containing 50 ml of acetic acid solution (0.05 M), which was placed on a magnetic stirrer for 30 min. The concentration of adsorbed acid was determined by titration of 10 ml of filtrate against NaOH (0.05 M) solution. Similarly the effect of AC weight on adsorption process was studied by taking 0.2, 0.25, 0.3 and 0.35 g of adsorbent.

Effect of adsorbent size and weight on adsorption is shown in Figure 3a and Figure 3b, it is clear that the adsorption efficiency of activated charcoal (BLRC, ZBLRC & MW BLRC) increases with decreasing carbon size and also increasing carbon weight. Finely divided carbon which is small in size exhibited more active sites and hence increase in amount of adsorption.

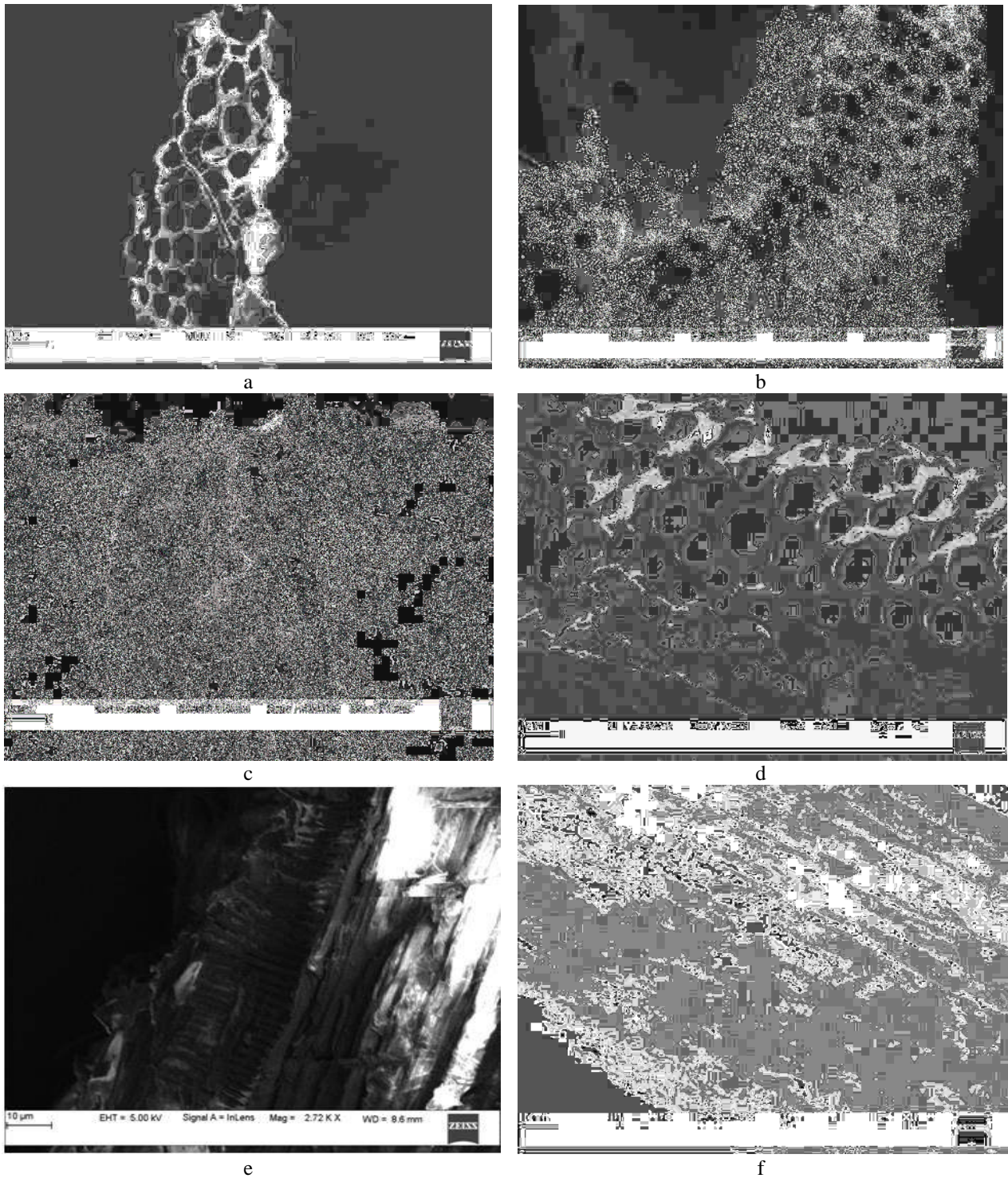


**Figure 2.** Activated carbon SEM images

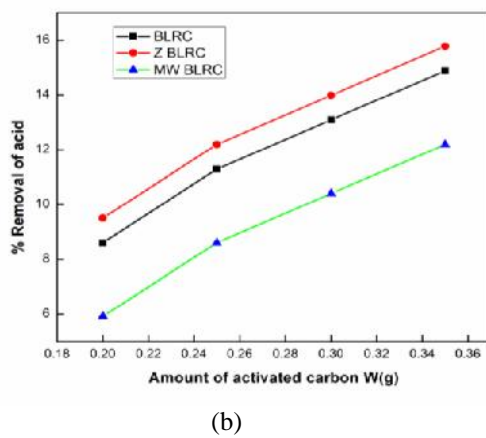
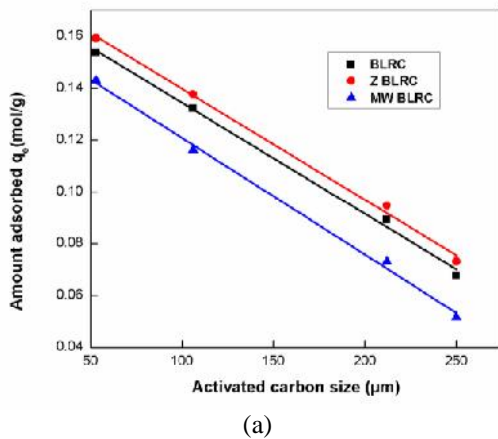


**Figure 3.** (a) Effect of AC size and (b) Effect of AC weight on adsorption of AA on (●) BLRC, (●) Z BLRC and (▲) MW BLRC

**Adsorption isotherm**

Adsorption of acetic acid on activated charcoal was also studied by varying the concentration of acetic acid solution (0.02 M, 0.03M, 0.04 M, 0.05 M and 0.06 M) at constant temperature (30 °C), activated carbon weight (0.25 g) and agitation time (30 min). Adsorption data was fitted to three types of adsorption isotherms namely Freundlich, Langmuir and Brunauer-Emmett-Teller (BET) adsorption isotherm to see which isotherm is the best suited for the present system.

The logarithmic form of empirical equation of Freundlich adsorption isotherm stated as follows [18]:

$$\log q_e = \log k_f + \frac{1}{n} \log C_e \tag{9}$$

Where  $k_f$  and  $n$  are the Freundlich constants for a given adsorbate and adsorbent at a particular temperature; which are helpful in finding the feasibility of adsorption process and there by comparing the adsorption efficiency of adsorbent. Where  $C_e$  is the concentration of acetic acid at equilibrium. A plot of  $\log q_e$  versus  $\log C_e$  was plotted (Figure 4(a).) The  $k_f$  and  $1/n$  values are calculated

respectively from the slope and intercept of the Freundlich isotherm plot and are shown in Table 2.

Langmuir adsorption isotherm equation [19] was also used in the present study; the expression stated as follows:

$$\frac{C_e}{q_e} = \frac{C_e}{q_m} + \frac{1}{q_m b} \tag{10}$$

Where  $C_e$  is concentration of acetic acid adsorbed at equilibrium,  $q_e$  is the amount of acetic acid adsorbed at equilibrium,  $q_m$  and  $b$  are Langmuir constants which indicates the monolayer adsorption capacity and the adsorption intensity of adsorbent. Linear plot observed for the plot of  $C_e/q_e$  versus  $C_e$  is shown in Figure 4(b). From the slope and intercept of the above linear plot, value of  $q_m$  and  $b$  can be calculated. Equilibrium parameter  $R_L$  was calculated and shown in Table 2.

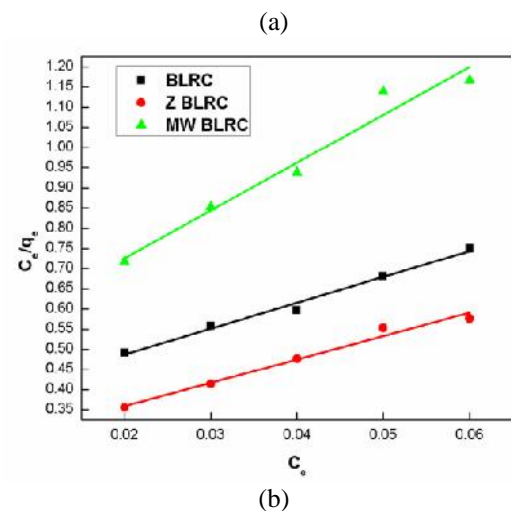
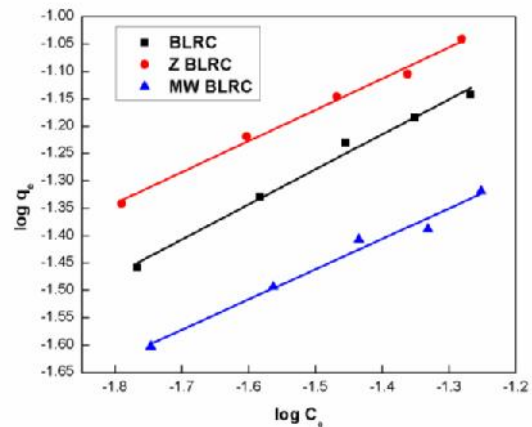


**Figure 4.** (a) Freundlich adsorption isotherm plot and (b) Langmuir adsorption isotherm plot of adsorption of AA on (●) BLRC, (●) Z BLRC and (▲) MW BLRC

An attempt was made to find out the possibility of formation of multilayer adsorption of AA on AC by applying the BET equation [20] stated as follows:

$$\frac{C_e}{(C_s - C_e)q_e} = \frac{1}{k_b q_m} + \left(\frac{k_b - 1}{k_b q_m}\right) \left(\frac{C_e}{C_s}\right) \quad (11)$$

Where  $C_e$  is the concentration of acid at equilibrium,  $C_s$  saturation concentration,  $q_m$  is the amount of acid required to form monolayer and  $k_b$  is the adsorption coefficient. The plot of  $\frac{C_e}{(C_s - C_e)q_e} V_s \frac{C_e}{C_s}$  was found to be nonlinear, it indicates the non-applicability of BET equation or the absence of multilayer adsorption of AA on AC. The value of Freundlich constant  $n$  for acetic acid - BLRC, Z BLRC and MW BLRC adsorption system is more than 1 and less than 10 which indicates adsorption is favorable. The RL value lies between 0 and 1 it confirmed the favorable adsorption. The  $R_2$  value is relatively higher for Freundlich adsorption isotherm in comparison with Langmuir adsorption isotherm. The heterogeneous adsorption of AA also found in SEM image (Figures 2b, 2d and 2f). Therefore, it can be believed that Freundlich adsorption isotherm fits well for the adsorption of AA onto three types of AC samples.

**TABLE 2.** Freundlich and Langmuir constants for adsorption of acetic acid onto BLRC, Z BLRC and MW BLRC

Samples	$n$	$k_f$	$B$	$R^2$	$R_L$	$q_m$ (mol/g)	$R^2$
BLRC	1.56	0.47	17.83	0.99	0.59	0.07	0.99
ZBLRC	1.76	0.48	23.86	0.99	0.53	0.09	0.97
MW BLRC	1.80	0.23	24.22	0.98	0.52	0.05	0.95

### Kinetics of adsorption

Two types of kinetic model namely first-order and second-order kinetic model were used to determine the rate constant for the present adsorption process. The following first-order (Eq. (12)) and second-order kinetic equation (Eq. (13)) [21] were used to calculate the kinetic parameters.

$$\log(q_e - q_t) = \log q_e - \frac{k_1 t}{2.303} \quad (12)$$

Where  $q_e$  is the amount of acetic acid adsorbed at equilibrium and  $q_t$  is the amount of acid adsorbed at time  $t$ ;  $k_1$  is the first order rate constant. A plot of  $\log(q_e - q_t)$  versus  $t$  was drawn and shown in Figure 5 (a). Second-order kinetics equation is as follows:

$$\frac{t}{q_e} = \frac{1}{k_2 q_e^2} + \frac{t}{q_e} \quad (13)$$

Where  $k_2$  is the second-order rate constant and it was calculated from the slope of linear plot  $t/q_t$  versus  $t$  as shown in Figure 5(b).

From Table 3 it is clear that the correlation coefficient value  $R^2$  of first order kinetic is smaller than that obtained for second order kinetic model. The second order rate constant  $k_2$  was calculated and shown in Table 3. Value of  $k_2$  varies from one carbon to another indicating the difference in mechanism of adsorption.

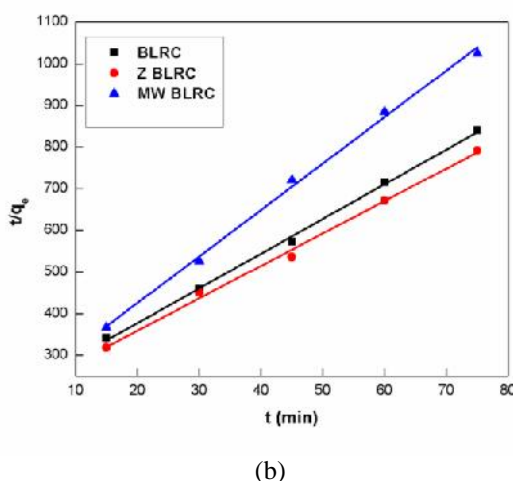
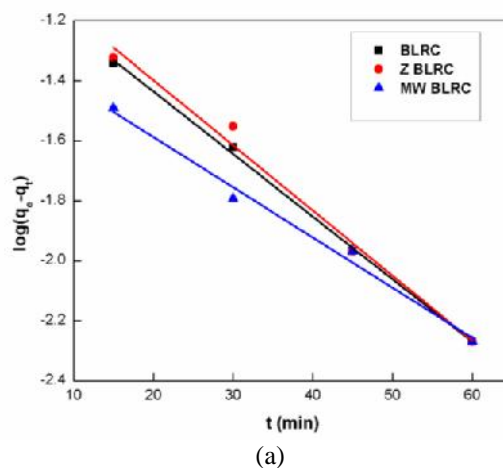


**Figure 5.** (a) First-order kinetic plot and (b) Second-order kinetic plot of adsorption of AA on (■) BLRC, (●) Z BLRC and (▲) MW BLRC

**TABLE 3.** First-order and second-order kinetic parameters of the adsorption of AA on BLRC, Z BLRC and MW BLRC

Samples	$k_1$ (min <sup>-1</sup> )	$q_e$ (mol/g)	$R^2$	$q_{max}$ (mol/g)	$k_2$ (mol.g/ min)	$q_e$ (mol/g)	$R^2$
BLRC	0.046	0.095	0.997	0.089	0.597	0.119	0.997
Z BLRC	0.049	0.108	0.983	0.095	0.550	0.128	0.995
MW BLRC	2.883	0.055	0.985	0.073	0.924	0.089	0.996

### Thermodynamics of adsorption

Thermodynamics of adsorption of acetic acid onto activated carbon was studied at temperature 15 °C, 30 °C, 45 °C and 60 °C with the condition of the system as stated earlier. Thermodynamic parameters such as energy of activation ( $E_a$ ), change in enthalpy ( $\Delta H^\ddagger$ ), entropy ( $\Delta S^\ddagger$ ) and free energy ( $\Delta G^\ddagger$ ) were evaluated using Arrhenius equation and absolute theory of rate expression as shown below [22]:

$$\log k = \log A - \frac{E_a}{2.303RT} \quad (14)$$

Where  $k$  is concentration of acid after adsorption,  $E_a$  is the activation energy,  $A$  is the Arrhenius parameter,  $R$  is gas constant and  $T$  is temperature (K). The values of  $E_a$  is calculated from the slope of linear plot of  $\log k$  versus  $1/T$  and is shown in Figure 6(a). Further the thermodynamic parameters like change in enthalpy, entropy and free energy were calculated using as follows:

$$\log\left(\frac{k}{T}\right) = \log\left(\frac{k_B}{h}\right) + \frac{\Delta S^\ddagger}{2.303R} - \frac{\Delta H^\ddagger}{2.303RT} \quad (15)$$

Where  $k_B$  is the Boltzmann constant,  $h$  is plank's constant. The change in enthalpy ( $\Delta H^\ddagger$ ) and change in entropy ( $\Delta S^\ddagger$ ) was calculated from the slope and intercepts of linear plot of  $\log(k/T)$  versus  $1/T$  as shown in Figure 6(b).

Change in free energy ( $\Delta G^\ddagger$ ) can be calculated using the Eq. (16)

$$\Delta G^\ddagger = \Delta H^\ddagger - T\Delta S^\ddagger \quad (16)$$

From the value of ( $\Delta G^\ddagger$ ) adsorption constant  $K_{ads}$  can be calculated from the equation :

$$\Delta G^\ddagger = -RT \ln K_{ads} \quad (17)$$

From Table 4, energy of activation was found to be negative in all the cases of activated carbons indicates that no energy is required for the process of adsorption it is instantaneous. The value of enthalpy of adsorption found to be negative and almost equal in all the activated carbon system this indicates the exothermic nature of adsorption. The negative value of change in entropy and positive value of free energy of system implies the non spontaneity of adsorption. The adsorption constant value  $K_{ads} > 0.97$ ; therefore, adsorption is favorable on the surface of the activated carbon.

**TABLE 4.** Thermodynamic parameters for the adsorption of AA on (•)BLRC, (●) Z BLRC and (▲) MW BLRC

Adsorbents	$E_a$ (kJ/mol)	$\Delta H^\ddagger$ (kJ/mol)	$\Delta S^\ddagger$ (J/mol/K)	$\Delta G^\ddagger$ (kJ/mol)	$K_{ads}$ (kJ/mol)
BLRC	-0.533	-3.103	-185.6	54.525	0.988
Z BLRC	-0.544	-3.115	-185.8	54.575	0.978
MW BLRC	-0.645	-3.216	-185.2	54.287	0.978

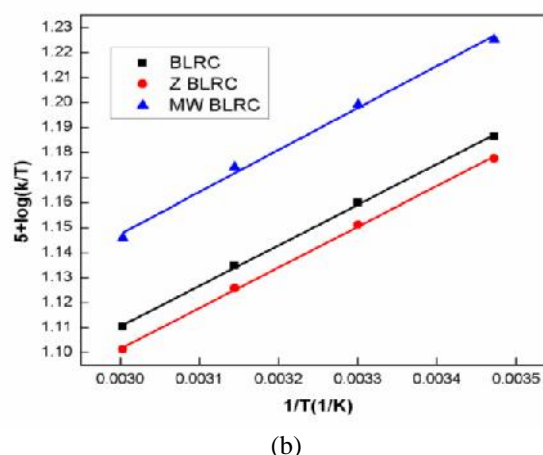
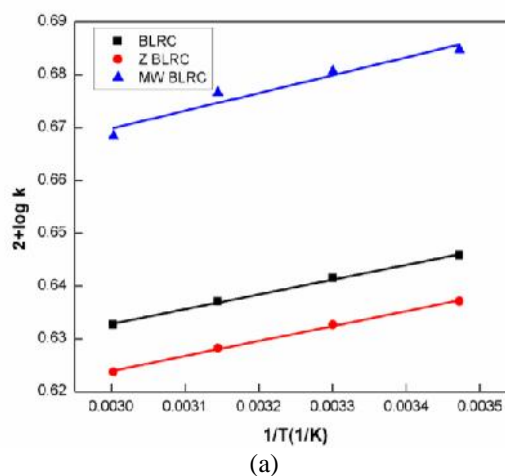


**Figure 6.** (a) Arrhenius plot of  $2+\log k$  Vs  $1/T$ , (b) Plot of  $5+\log(k/T)$  Vs  $1/T$

## CONCLUSION

The Freundlich adsorption isotherm holds good for the adsorption of acetic acid onto activated charcoal (BLRC, Z BLRC & MW BLRC). The present adsorption process followed the second order kinetics. Evaluation of thermodynamic parameters such as change in enthalpy ( $\Delta H^\ddagger$ ), change in entropy ( $\Delta S^\ddagger$ ) & change in free energy ( $\Delta G^\ddagger$ ) results exothermic and non spontaneous nature of adsorption. Hence the characterization and adsorption studies both reveal that chemical activated charcoal has more adsorption capacity than physical and microwave activated charcoal.

## Acknowledgements

The authors are thankful to the co-ordinator, DST-FIST program, USIC and DST-PURSE, Mangalore University for providing instrumental facilities to carry out the present research work. The authors are also thankful to

UGC-SAP, Delhi for financial assistance to carry out the present research work.

## REFERENCES

- Basile, A., Acetic acids: Chemical Properties, Production and Applications 2003: Nova Science.
- Sawyer, C.N., P.L. McCarty and G.F. Parkin, 2003. Chemistry for environmental engineering and science.
- Daifullah, A., B. Girgis and H. Gad, 2003. Utilization of agro-residues (rice husk) in small waste water treatment plants. Materials letters, 57(11): 1723-1731.
- Reinoso, H.M.a.F.R., Activated carbon 2007: Elsevier Ltd.
- Ilaboya, I., E. Oti, G. Ekoh, L. Umukoro and A. Ibiam, 2013. Performance of activated carbon from cassava peels for the treatment of effluent wastewater. Iranica Journal of Energy and Environment, 4(4): 361-370.
- Mohammad, Y., E. Shaibu-Imodagbe, S. Igboro, A. Giwa and C. Okuofu, 2014. Adsorption of phenol from refinery wastewater using rice husk activated carbon. Iranica Journal of Energy & Environment, 5(4): 393-399.
- P. Chaithra, K.H.a.J.I.B., 2016. An Investigation on the Attack of Dye Species on Freshly Synthesized and Characterized Activated Carbon from Cocoa pod. Iranica Journal of Energy and Environment, 7(4): 350 - 358.
- Mahmoudi, K., N. Hamdi and E. Srasra, 2014. Preparation and characterization of activated carbon from date pits by chemical activation with zinc chloride for methyl orange adsorption. J. Mater. Environ. Sci, 5(6): 1758-1769.
- Srinivasan, T. and G. Vijayalakshmi, 2011. Biomangement of banana leaf waste through microbial technology. Journal of Applied Environmental and Biological Sciences, 1(7): 126-128.
- Sugumaran, P., V.P. Susan, P. Ravichandran and S. Seshadri, 2012. Production and characterization of activated carbon from banana empty fruit bunch and Delonix regia fruit pod. Journal of Sustainable Energy & Environment, 3(3): 125-132.
- Abdullah, N., F. Sulaiman, M.A. Miskam and R.M. Taib, 2014. Characterization of banana (Musa spp.) pseudo-stem and fruit-bunch-stem as a potential renewable energy resource. International Journal of Biological, Veterinary, Agricultural and Food Engineering, 8(8): 712-716.
- Ramakrishnan, K. and C. Namasivayam, 2011. Zinc chloride-activated jatropha husk carbon for removal of phenol from water by adsorption: equilibrium and kinetic studies. Toxicological & Environmental Chemistry, 93(6): 1111-1122.
- P. Chaithra and J.I. Bhat, P.I.c., 2016. Its characterization and capacity as an adsorbent towards H+. Journal of Chemical and Pharmaceutical Research, 8(8): 706-715.
- Prahas, D., Y. Kartika, N. Indraswati and S. Ismadji, 2008. Activated carbon from jackfruit peel waste by H<sub>3</sub>PO<sub>4</sub> chemical activation: pore structure and surface chemistry characterization. Chemical Engineering Journal, 140(1): 32-42.
- Khan, Z.R., M.S. Khan, M. Zulfequar and M.S. Khan, 2011. Optical and structural properties of ZnO thin films fabricated by sol-gel method. Materials Sciences and applications, 2(05): 340.
- Xiao, L.-P., Z.-J. Sun, Z.-J. Shi, F. Xu and R.-C. Sun, 2011. Impact of hot compressed water pretreatment on the structural changes of woody biomass for bioethanol production. BioResources, 6(2): 1576-1598.
- Lehninger, A., Glycolysis: a central pathway of glucose catabolism. Principles of biochemistry, 1984, Worth Publishers, New York.
- Prabakaran, R. and S. Arivoli, 2012. Thermodynamic and isotherm analysis on the removal of malachite green dye using thespesia populnea bark. Journal of Chemistry, 9(4): 2575-2588.
- Sawasdee, S. and P. Watcharabundit, 2015. Equilibrium, Kinetics and Thermodynamic of Dye Adsorption by Low-Cost Adsorbents. International Journal of Chemical Engineering and Applications, 6(6): 444.
- Harish, R.C.G.a.C.M., 1982. Adsorption and Phase rule. Goel.
- Zhang, H., Y. Wang, P. Bai, X. Guo and X. Ni, 2015. Adsorptive separation of acetic acid from dilute aqueous solutions: adsorption kinetic, isotherms, and thermodynamic studies. Journal of Chemical & Engineering Data, 61(1): 213-219.
- Karaoglu, M.H., Ş. Zor and M. Uğurlu, 2010. Biosorption of Cr (III) from solutions using vineyard pruning waste. Chemical Engineering Journal, 159(1): 98-106.

## Persian Abstract

DOI: 10.5829/idosi.ijee.2017.08.01.07

### چکیده

ذغال فعال از لبه برگ موز به سه روش فعالسازی فیزیکی، فعالسازی شیمیایی (ZnCl<sub>2</sub>) و فعالسازی با استفاده از مایکروویو سنتز شد. ذغال فعال با استفاده از آنالیز میکروسکوپ الکترونی روبشی گسیل میدانی (FE-SEM) و آنالیز پراش اشعه X (XRD) شناسایی شد. ذغال فعال سنتز شده به روش شیمیایی جاذب بهتری نسبت به ذغال فعال سنتز شده با دو روش فیزیکی و با استفاده از مایکروویو بود. جذب سطحی اسید استیک بر روی هر سه ذغال فعال انجام شد. داده‌های تجربی با معادلات جذب ایزوترم فروندلیش تطابق داشت. سینتیک مرتبه دوم برای سیستم جذب فعلی بررسی شد. پارامترهای ترمودینامیکی مورد ارزیابی قرار گرفت. بر اساس نتایج می‌توان نتیجه گرفت که ذغال فعال شده به روش شیمیایی حداکثر بازده جذب را در میان سه نوع کربن فعال سنتز شده دارد.